AN EXPERIMENTAL STUDY OF INTUMESCENT FIRE PROTECTION COATINGS

Mesquita, L.M.R. [1]; Piloto, P.A.G. [1]; Vaz, M.A.P. [2]
[1] – Applied Mechanics Dep., Polytechnic Institute of Bragança, 5300-857 Bragança, Portugal.
[2] – DEMEGI-FEUP, University of Porto, Rua Dr Roberto Frias S/N, 4200-465 Porto Portugal.

ABSTRACT

The use of intumescent coatings plays an important role in the fire protection of structural elements. When submitted to elevated temperatures an intumescent coating undergoes thermochemical reactions that promote a higher thermal protection. To evaluate the behaviour of an intumescent coating, a set of experimental tests made on coated steel plates are performed in a cone calorimeter. These tests are performed with different heat fluxes and intumescent thicknesses. A simple and an advanced model, based in the Finite Difference Method, are presented and applied to determine the intumescent surface temperature evolution, considering the initial thickness and the intumescence variation.
The intumescence effective thermal conductivity is estimated by solving the inverse heat transfer problem, considering the temperature in the steel equal to the experimental measured values. When the intumescence thickness variation is taken into account in the numerical model a higher thermal conductivity is expected, when compared with the constant thickness model.

1 INTRODUCTION

The use of fire protection materials is one of the measures normally adopted to prescribe structural fire resistance. Critical temperature of protected structural elements is one of the main design parameters and depends essentially on the protection material properties and on the bulk fire temperature. Passive fire protection materials insulate steel structures from the effects of the elevated temperatures that may be generated during fire. They can be divided into two types, non-reactive, of which the most common types are boards and sprays, and reactive, being intumescent coatings an example.
The intumescent coating behaviour is characterized by expansion and mass loss, producing a foam char with a volume that varies from 5 to 200 times its original volume. Heat transfer analysis through the protection material, during the initial stage and its intumescence, assumes great importance to define and design this thermal protection.
The problem to determine the temperature field in an intumescent material involves the solution of a phase transformation problem with two ore more moving boundaries that characterize its state, initial, softened and carbonaceous char.
Different models handle the intumescent behaviour with char forming polymers as a heat transfer problem. Other existing models provide a suitable description regarding the intumescence and char formation using kinetic studies of thermal degradation, accounting the complex sequence of chemical reactions, thermal and transport phenomenon, [1-4].
Due to the thermal decomposition complexity of intumescent coating systems, the models presented so far are based on several assumptions, being the most relevant the consideration of one-dimensional heat transfer trough material, temperature and space independent thermal properties and the assumption of a constant incident heat flux where the heat losses by radiation

and convection are ignored, [2]. Thermochemical processes of intumescence also occur without energy release or energy absorption, [5].
Anderson et al, [6,7], developed a mathematical model which describes the mechanism of intumescence by considering the mass and energy conservation equations, assuming the heat rate per unit mass generated by chemical reactions mainly at the pyrolysis zone and the heat due to the outgassing of volatile products. The intumescence was accounted considering the mass loss during the process. The model assumes that the transition to the intumescent state occurs at a very thin zone or front and is divided into two regions, the virgin material and the char layers. This model is compared with experimental results performed in steel plates coated with intumescent paints. Later, in [8], Anderson et al present an estimate for the effective char thermal conductivity. The results show that the insulation efficiency of the char depends on the cell structure and the low thermal conductivity of intumescent chars result from the pockets of trapped gas within the porous char which act as a blowing agent to the solid material.
The authors, in a previous work [9], carry out several full scale fire resistant tests to determine the behaviour of steel members protected with intumescent coatings, considering different dry film thicknesses. Based on the results the intumescent effective thermal conductivity temperature variation was estimated. All properties modification, physical and thermal, was implicitly accounted.
This work presents an experimental and numerical study based on steel plates coated with intumescent paint and subjected to a radiant heat flux inside a cone calorimeter in well-controlled conditions. The intumescence thickness and steel temperatures are measured experimentally and used later in the numerical study to assess the intumescence surface temperature and effective thermal conductivity.

2 EXPERIMENTAL TESTS

The intumescent chemistry has changed little over the past years and almost all coatings are largely based on the presence of similar key components: a dehydrating agent, a carbonaceous source, a spumific and a binder resin. The first reaction that occurs is the decomposition of the dehydrating agent, usually ammonium polyphosphate, into ammonia and phosphoric acid. At higher temperatures, between 200-300 [ºC], the acid reacts with the carboniferous agent. The formed gases will expand, beginning the intumescence in the form of a carbonaceous char.
The coating performance is directly related to the time or temperature at witch the intumescence begins and how long it acts as a thermal barrier.
To assess the performance of an available water-based commercial intumescent paint three experimental tests are presented. These tests are conducted in a cone calorimeter which enabled the determination of the heat release rate, mass loss rate, effective heat of combustion, ignitability and extinction during the combustion of samples.
The steel plates are 100 [mm] squared and 4 [mm] thick, coated in one side with different dry film thicknesses and tested in a cone calorimeter as prescribed by the standard E1354-04, [10]. Temperatures are measured by means of four thermocouples, type k, welded at the plate in the heating side and at the opposite side, at two different positions, see Figure 1.

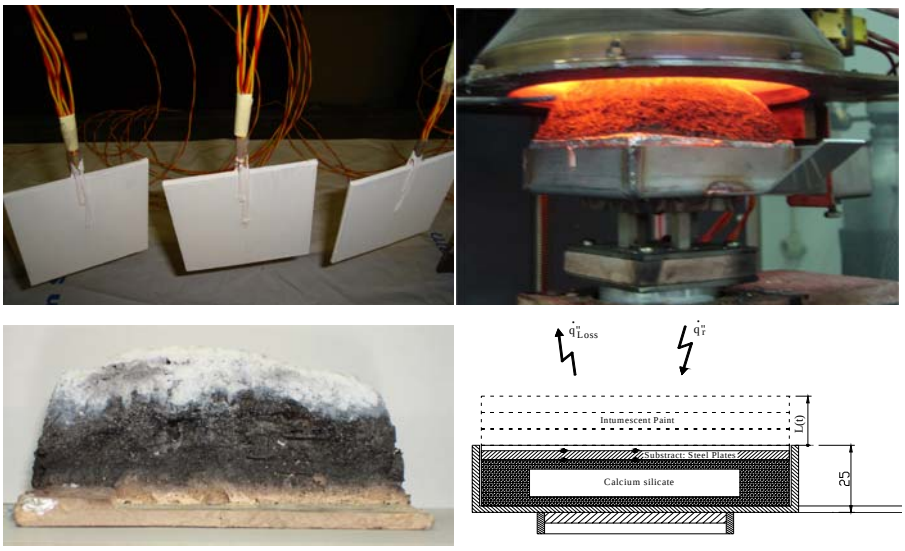

Fig. 1 – Steel plates coated, with fixed thermocouples, cone calorimeter setup and intumescence development.

The specimens were wrapped with aluminium foil and placed in the sample holder with its bottom lined with a layer of calcium silicate adjusted to place the specimen top surface in correct position.

Although the cone calorimeter test standard specifies that the sample surface for deforming or intumescent systems be fixed by using a retainer frame and wire grid, this "special mounting" was not used. It should be noted that this procedure has been criticized because the prevention of intumescence changes the coating performance and was never well accepted by the scientific community, [11].

The distance between the sample surface and the heater remained unchanged, at approximately 25 [mm], which means that with the increasing intumescence the top of the sample came closer to cone. This could bring some non uniformity to the heat flux at the sample surface, mainly on the edge, as experienced in the Schartel et al work, [11].

The mean value of 23 measured dry film thicknesses are 3010, 2680 and 2690 [μm] for the three specimens, and the exposed thermal radiation in the cone calorimeter was fixed to 75, 25 and 25 [kW/m^2], for the test1, test2 and test3 respectively. These radiant heat fluxes are representative of an initial fire stage and a well developed fire.

2.1 Experimental Results

The tests were executed through 1200 [s] and during this period the intumescence growth was recorded with a camera. At the end of all tests, the intumescence exceeds the cone base level. The final maximum intumescence, measured after each test, was 41.74, 29.50 and 35.36 [mm] for the test 1, 2 and 3, respectively.

The heat release rate and the effective heat of combustion of test 1 and 2 were approximately zero. Test1 registered a heat release rate peak value of 26.3 [kW/m^2] for time equal to 155 [s], an effective heat of combustion peak value of 17.1 [MJ/kg] at time 200 [s], with average values of 9.8 [kW/m^2] and 8.3 [MJ/kg], respectively. These values are very small and can be considered negligible.

Transient flames were registered in test1 between instants 80 and 125 [s], and enter in combustion after 130 [s] up to 730 [s].
Figure 1 represents mass loss and residual weight of all tests. During all tests the mass loss is almost linearly proportional to time, presenting test1 higher reduction, about 41.5 %, compared with the other two, about 11.5%.

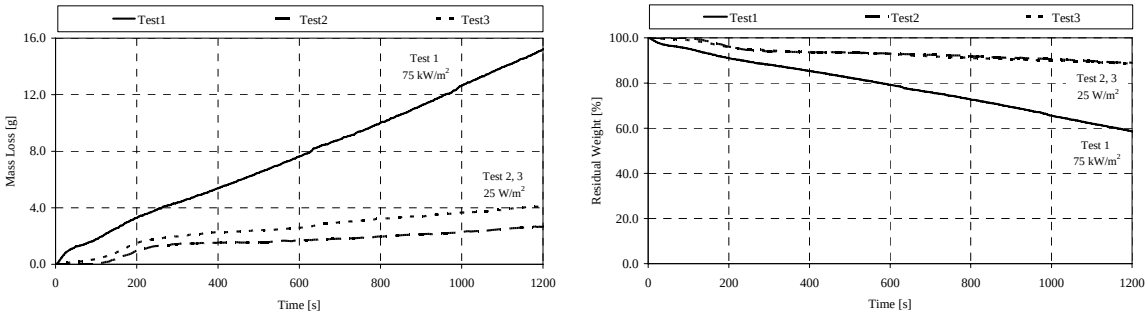

Fig. 2 – Measured mass loss and residual weight.

Using discrete frames obtained from the camera during tests and by image processing techniques, the intumescence development was measure over time, see figure 3. Due to the high intumescence during test 1, boundary development measurement was limited to the visual space, not allowing useful images till the end of the test.

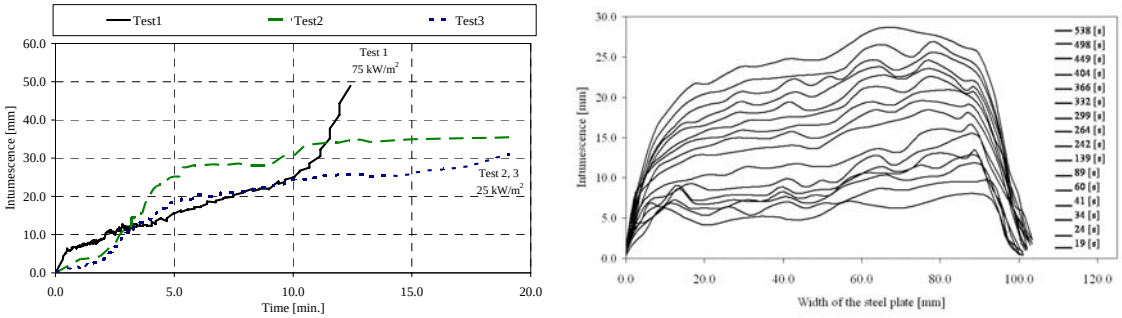

Figure 3 – Measured intumescent thickness variation and planar intumescence profile of test1.

Figure 3 also represents the intumescent development (free boundary) of test1 in the sample vertical plane. Higher intumescence may be noticed in sample right region coincident to the thermocouples wire position responsible for coating accumulation.
Temperature profiles measured at the interface intumescent coating and substrate are reported in figure 4. Measured values from the thermocouples welded on the bottom of the plate are very close to the temperatures at the top. As expected, temperatures resulting from test1 are higher than temperatures obtained from the other tests.

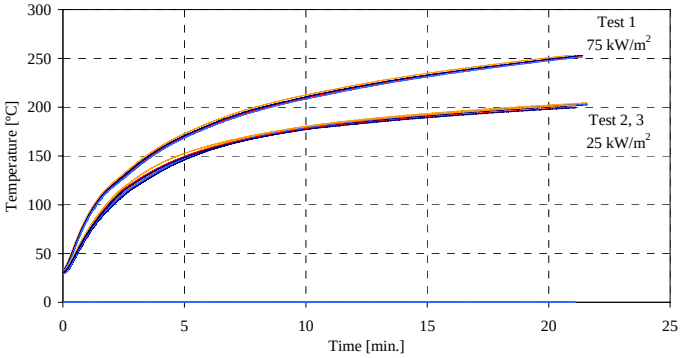

Fig. 4 – Measured temperatures at top and bottom of the steel plate.

3 NUMERICAL STUDY OF INTUMESCENCE BEHAVIOUR

When intumescent coating is exposed to an external heat flux it starts to react, initiating the intumescing process. These reaction mechanisms include an initial stage of preheating where thermal energy is absorbed by the coating and its temperature increases quickly. When the temperature at the virgin coating surface reaches the pyrolysis temperature, some heat is absorbed by the coating in an endothermic process, and gas bubbles are formed that originates the growth of a black carbonaceous char. As the thermal wave develops through the virgin material the carbonaceous char keeps growing until the moving front reaches the substrate and all the virgin coating is consumed, as represented in figure 5.

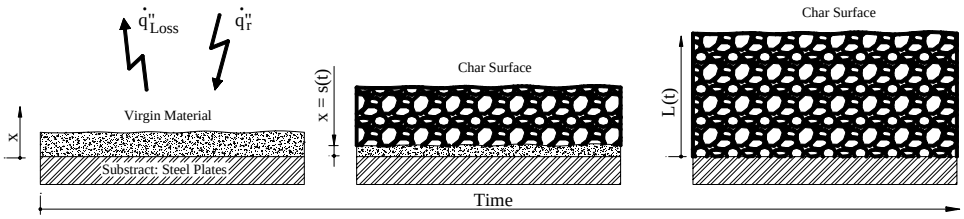

Fig. 5 – Development of the intumescence.

In all models presented so far the transition region, from virgin to char, is considered to occur in an infinitesimally thin front, as proposed by Anderson et al, [7].
The problem of solving energy equation on each side of the moving boundary is considered as a generalized Stefan problem, in which the moving boundary and the free boundary locations must be determined as part of the proposed problem.

3.1 Approximate solution for intumescence surface temperature

An exact prediction of the intumescence surface temperature is very complex to achieve because it must consider the exact amount of heat flux that arrives to the surface, and because thermal behaviour of the intumescent coating should be characterized. Acquaintance of thermal properties (thermal conductivity, etc.) is decisive, the influence of the substrate and the heat losses through the back surface represents some of the major difficulties for the numerical process.

At the present state an approximate solution is used, where the heat balance equation is defined by the equation 1, [12].

$$\varepsilon \dot{q}_r^{"} - \dot{q}_{r,L}^{"} - \dot{q}_{conv,L}^{"} = c_i \rho_i d_i \frac{\partial T}{\partial t} + c_s \rho_s d_s \frac{\partial T}{\partial t} \quad (1)$$

In this equation $\dot{q}_r^{"}$ represents the radiant heat flux emitted by the cone calorimeter, $\dot{q}_{r,L}^{"}$ and $\dot{q}_{conv,L}^{"}$ represent the heat loss at the surface by radiation, $\varepsilon\sigma\left(T^4 - T_a^4\right)$, and heat loss by convection, $h_c\left(T - T_a\right)$, respectively. The first and second term on the right hand side of equation (1) represent the heat stored at the intumescent coating and at the steel plate. In this equation the endothermic and exothermic processes are ignored. Additionally as the measured steel temperatures are very close, at the top and bottom of the steel plate, we do not consider any small heat loss through the bottom of the steel plate. ε represent the surface emissivity of the intumescent coating, σ is the Stefan-Boltzmann constant, h_c is the convective heat transfer coefficient. ρ, c and d represents the density, specific heat and thickness, respectively. The subscripts i and s represent the intumescent coating and steel material properties, respectively.
Generally the emissivity is temperature dependent and varies as a function state of the material. For intumescent materials values between 0.7 and 0.95 can be found in the literature, where the lower value is normally used for the virgin material state, [13], and values of 0.8, 0.9 and 0.95 are used for the intumescence char surface, see [8,13,14]. In this work an emissivity value of 0.9 and a constant convective heat transfer coefficient equal to 20 [W/(m^{2}K)] are considered.
The intumescent coating specific mass was measured by the pycnometer method given a value of 1375 [kg/m^3] for the virgin coating and a value of 616 [kg/m^3] for the char material. It should be aware that this method does not account for material porosity.
The solution of equation (1) is obtained by the finite difference method, where the time derivative of temperature is approximated by a forward finite difference, resulting in the equation (2).

$$\varepsilon \dot{q}_r^{"} - h_c\left(T_t - T_a\right) - \varepsilon\sigma\left(T_t^4 - T_a^4\right) = \frac{\left(c_i \rho_i d_i\right)_{t+\Delta t}}{\Delta t}\left[\frac{T_{t+\Delta t} + T_{st}}{2} - \frac{T_t + T_{st}}{2}\right] + \frac{c_s \rho_s d_s}{\Delta t}\left[\frac{T_{st+\Delta t} - T_{st}}{2}\right] \quad (2)$$

Here T_s represents the steel temperature. The temperature of the intumescent coating is assumed to be the average value of its free surface temperature and the steel temperature. In the same way, steel temperature was considered as the average value of the top and bottom measured steel temperatures.
Steel properties are assumed constant, with a specific heat value of 600 [J/kgK] and a specific mass equal to 7850 [kg/m^3]. The intumescent coating specific heat was considered constant and equal to 1000 [J/kgK].
Figure 6 presents the intumescence coating surface temperatures for two studied cases. In the first case, C1, the specific mass of the virgin material and a constant thickness equal to the initial dry coating thickness were considered. In the second case, C2, the specific mass and the intumescent thickness were considered time dependent. An average value for intumescence thickness of test1 and test2 was considered.

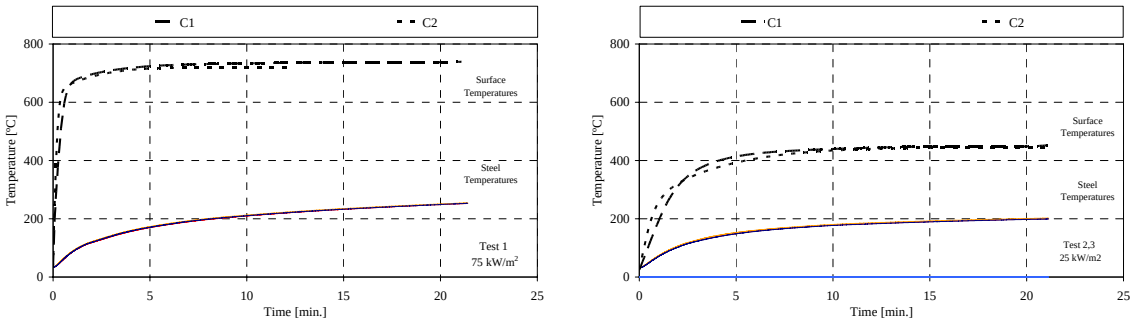

Fig. 6 - Determined intumescence surface temperatures.

Figure 6 shows that, at the initial stage, the heat stored in the intumescent coating has a large influence in the surface temperature. The higher surface temperatures at the beginning of the test, verified in the case C2, are due to the reduced heat stored considered when the char specific mass is used.

3.2 Determination of the effective thermal conductivity

The development of the intumescence may be treated as a one-dimensional heat conduction problem, where the heat flows through the coating layer and, assuming that the transition between virgin and char takes place in a very thin layer, it starts to be active at a temperature T^*. After this preheating phase, the surface reaches the transition temperature and the coating is divided into two layers: the virgin and the char layers. In order to determine an estimation of the intumescence effective thermal conductivity, a unique layer of constant specific mass and constant specific heat was assumed. The governing equation for the problem is:

$$c\rho\frac{\partial T}{\partial t} = k_{eff}\frac{\partial}{\partial x}\frac{\partial T}{\partial x} \qquad 0 < x < L(t) \tag{3}$$

The boundary condition at the free surface requires that the heat flux that enters in the char is equal to the heat that arrives from the cone minus the heat losses by convection and radiation.

$$k_{eff}\left.\frac{\partial T}{\partial x}\right|_{x=L(t)} = \varepsilon\dot{q}_r^{"} - h_c\left(T - T_a\right) - \varepsilon\sigma\left(T^4 - T_a^4\right) \qquad x = L(t) \tag{4}$$

For the boundary condition at the coating and substrate interface, $x = 0$, due to the large diffusivity and low thickness of the steel plates, no temperature gradient was considered over the plate. Assuming an adiabatic condition on the back of the substrate, the boundary condition is defined by equation (5).

$$k_{eff}\frac{\partial T}{\partial x} = d_s c_s \rho_s \frac{\partial T_s}{\partial t} \qquad x = 0 \tag{5}$$

The initial conditions are given by equations (6) and (7).

$$L(0) = d_0 \tag{6}$$

$$T(x,0) = T_a \tag{7}$$

The problem of estimate K_{eff} and the temperature field $T(x,t)$ as formulated by the equations 3-7, is inverse ill-posed since it will not, in general, have a unique solution, [15]. To solve this problem additional constraints on the temperature are required. We assume that the steel temperature is known and equal to the experimental measured values given in the figure 4.

$$T_s(0,t) = T_s(t) \tag{8}$$

Applying a backward finite difference scheme for approximating the time derivative and after the boundary conditions specifications, the temperature field and the effective thermal conductivity are determined by equations (9-11).

For $i = 1 \quad , \quad x = 0$

$$c\rho_{i,k-1}\frac{T_{i,k} - T_{i,k-1}}{\Delta t} = \frac{1}{\Delta x_i}\left[k_{eff,k}\frac{T_{i+1,k} - T_{i,k}}{\Delta x_i} - d_s c_s \rho_s \frac{T_{i,k} - T_{i,k-1}}{\Delta t}\right] \tag{9}$$

For $1 < i < n_x \quad , \quad 0 < x < L(t)$

$$c\rho_{i,k-1}\frac{T_{i,k} - T_{i,k-1}}{\Delta t} = \frac{1}{\Delta x_i}\left[k_{eff,k}\frac{T_{i+1,k} - 2T_{i,k} - T_{i-1,k}}{\Delta x_i}\right] \tag{10}$$

For $i = n_x \quad , \quad x = L(t)$

$$c\rho_{i,k-1}\frac{T_{i,k} - T_{i,k-1}}{\Delta t} = \frac{1}{\Delta x_i}\left[\varepsilon\dot{q}_r^{"} - h_c\left(T_{i,k-1} - T_a\right) - \varepsilon\sigma\left(T_{i,k-1}^4 - T_a^4\right) - k_{eff,k}\frac{T_{i,k} - T_{i-1,k}}{\Delta x_i}\right] \tag{11}$$

The calculation starts at node $i = 1..n_x$ and at instant k assuming a constant initial thermal conductivity. The temperature field is determined by solving the system by the standard LU decomposition method. An iterative procedure is applied to refine the thermal conductivity value, with a stopping criteria of $error = \left(T_{s,Exp} - T_{s\_num}\right)/T_{s,Exp} \le 1\%$. This value is used in the next time increment, which is determined accordingly to the stability condition $\Delta t = \Delta x^2/2\alpha$, and then a new effective thermal conductivity is obtained.

Figures 7 and 8 present the effective thermal conductivity numerical results for test1 and tests 2, 3, respectively, considering two cases C1 and C2, as described in the previous section. The figures also present the temperature in the intumescence surface, T_{surf}, and the steel temperature, T_{steel}, determined by this numerical method.

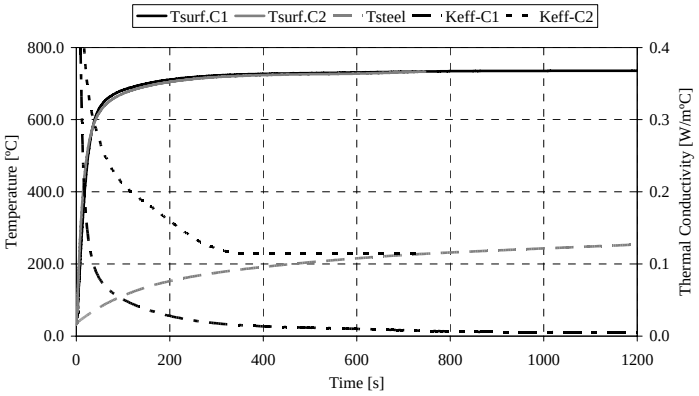

Fig. 7 – Effective thermal conductivity of test1.

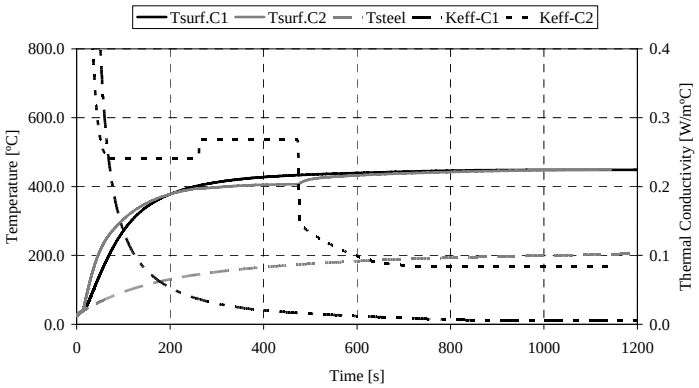

Fig. 8 – Effective thermal conductivity of test2 and 3.

The figures show that, at the initial stage of heating, the effective thermal conductivity decreases, until the surface and steel temperatures are approximately constant, and then a convergence to a constant value is achieved. The behaviour in both cases is similar and when the intumescence specific mass and thickness variation are accounted (C2), a higher thermal conductivity is obtained.

At final stage of the test a relatively higher difference was obtained between the cases C1 and C2, with values of 0.0056 [W/mºC] and 0.1151 [W/mºC] for test1 and 0.0053 [W/mºC] and 0.085 [W/mºC] for test1, 2, respectively.

4 CONCLUSIONS

This paper has presented a set of experimental tests conducted in a cone calorimeter to assess the intumescent coating behaviour when used in fire protection. The experimental tests show that the intumescence development depends on the initial dry thickness and on the incident heat flux. In the time interval of test the material residual weight is approximately linear.

A simple approximate solution to determine the intumescence surface temperature was presented and compared with an advanced numerical method. This numerical method is based in the finite difference method and was applied to estimate the intumescence effective thermal conductivity. Surface temperatures determined with both methods agree.

The effective intumescence thermal conductivity was determined considering the intumescence thickness variation and a constant thickness, equal to the initial, giving the first case a higher value in comparison to the second.

ACKNOWLEDGMENTS

The authors acknowledge the financial support from the Portuguese Science and technology Foundation, project PTDC/EME-PME/64913/2006, "Assessment of Intumescent Paint Behaviour for Passive Protection of Structural Elements Submitted to Fire Conditions", and fellowship SFRH/BD/28909/2006.

REFERENCES

[1]. Staggs J. E. J., "A discussion of modelling idealised ablative materials with particular reference to fire testing", Fire Safety Journal, Vol. 28, ,47-66, 1997.
[2]. Moghtaderi B., Novozhilov V., Fletcher, D., Kent J. H., "An integral model for the transient pyrolysis of solid materials" Fire and Materials, Vol. 21, 7-16, 1997.
[3]. Lyon R. E., "Pyrolysis kinetics of char forming polymers", Polymer Degradation and Stability, Nº 61, pp. 201-210, 1998.
[4]. Jia F., Galea E. R., Patel M. K., "Numerical Simulation of the Mass Loss Process in Pyrolizing Char Materials", Fire And Materials, Nº 23, 71-78, 1999.
[5]. Kuznetsov, G. V., Rudzinskii, V. P., "Heat transfer in intumescent heat- and fire-insulating coatings", Journal of Applied Mechanics and Technical Physics, Vol. 40, No. 3, 1999.
[6]. Anderson, C.E.; Wauters, D.K.;" A Thermodynamic Heat Transfer model for Intumescent systems", Int. Journal of Engineering Science, Vol. 22, Nº 7, pp.881-889, 1984.
[7]. Anderson, C.E.; Dziuk, J.; Mallow, W.A.; Buckmaster, J.; "Intumescent Reaction Mechanisms", Journal of Fire Sciences, Nº 3, 161-194, 1985.
[8]. Anderson, C.E.; Ketchum, D.E., Mountain, W.P. "Thermal Conductivity of Intumescent Chars", Journal of Fire Sciences, vol. 6, pp. 390, 1988.
[9]. Mesquita, L.M.R.; Piloto, P.A.G.; Vaz, M.A.P; Vila Real, P.M.M.; "Fire resistance tests in steel beams protected with intumescent coatings" (in portuguese); 6th National Congress for Experimental Mechanics; vol. 12, pp 129-137, ISSN 122 922, 2006.
[10]. E1354-04, Standard Test For Heat And Visible Smoke Release For Materials And Products Using An Oxygen Consumption Calorimeter, American Society For Testing And Materials, 2004.
[11]. Schartel B., Bartholmai M., Knoll U., "Some comments on the use of cone calorimeter data", Polymer Degradation and Stability, Nº 88, pp. 540-547, 2005.
[12]. A. Omranea, Y.C. Wang, U. Göranssonc, G. Holmstedt, M. Alden; "Intumescent coating surface temperature measurement in a cone calorimeter using laser-induced phosphorescence", Fire Safety Journal, 42, pp. 68–74, 2007.
[13]. Koo, J. H., "Thermal characterization of a ceramic intumescent material", Fire Technology, Vol. 34, Nº 1, 1998.
[14]. M. Bartholmai, R. Schriever, B. Schartel, "Influence of external heat flux and coating thickness on the thermal insulation properties of two different intumescent coatings using cone calorimeter and numerical analysis", Fire and Materials, Vol. 27, Issue 4, 151 – 162, 2003.
[15]. Al-Khalidy, N, "On the solution of parabolic and hyperbolic inverse heat conduction problems", International Journal of Heat and Mass Transfer, vol. 30, pp. 3731-3740, 1998.